AIAA JOURNAL
Vol. 32, No. 11, November 1994

Mechanical System Reliability and Risk Assessment

T. A. Cruse,* S. Mahadevan,† Q. Huang,‡ and S. Mehta§
Vanderbilt University, Nashville, Tennessee 37235

A new methodology is reported for the prediction of the reliability of mechanical structures subject to multiple failure modes, including noncritical damage. The reduction of system reliability due to accumulated damage is quantitatively estimated by updating the critical system failure states at each level of damage. Correlated design variables are automatically accounted for in the system reliability calculations. Second-order reliability bounds are reported which are unbiased to the ordering of the events. A system risk assessment methodology is also reported that accounts for the cost of multiple types of failure modes and includes the effect of inspection success on reducing the consequences of system failure. Application of the new technology is illustrated for a simplified system model of an aeropropulsion rotor system. However, the methodology is general and is applicable to any engineering system.

Nomenclature

A	= fatigue life coefficient
a_i	= initial crack size
a_{ij}	= linearization coefficients for response surface
b	= fatigue exponent
C	= crack growth rate coefficient
D_i	= design response function
E	= modulus
E_i^{Λ}	= failure event: i; level: Λ
$\boldsymbol{e}_j$	= system random variable unit vector
F_{tu}	= tensile ultimate strength
$g_i(\boldsymbol{x})$	= response function of independent random variables $\boldsymbol{x}$
K_{IC}	= critical stress intensity factor
N_{FM}	= fracture mechanics life
N_{LCF}	= fatigue life
n	= crack growth rate exponent
$P(\ )$	= probability
P_S^{CRIT}	= probability of system failure: critical mode
$RB, FB, FR, \ldots$	= failure mode symbols
S_i	= standard normal variable
x_i	= independent random design variables
β	= reliability index
Δ	= joint reliability index
ΔT	= temperature difference
δ_{INT}	= interference fit
μ	= mean value
ρ	= density; correlation parameter
σ	= standard deviation
Φ	= standard Gaussian distribution function
$\vec{\Phi}$	= system failure vector
ϕ_j	= system response location vector
Ω	= rotor speed

I. Introduction

THE reliability of a mechanical system may be defined as the probability of safe and successful performance of the system. A practical system has many different criteria for measuring safety and performance, and limit states are defined corresponding to each criterion. The violation of these limit states impacts the system with varying degrees of severity, ranging from mild reduction in the performance efficiency to total system failure. Thus the failure modes can be divided into two groups: 1) "critical" modes, which result in total failure of the system (e.g., fracture from an initial crack, burst from ultimate tensile failure, high-cycle fatigue due to resonance in turbomachinery, etc.); and 2) "noncritical" modes which degrade the system, resulting in changes in external load, internal stiffness, or part integrity (e.g., part yield or creep, part disengagement causing loss of preload or damping, low-cycle fatigue crack initiation to a crack size, etc.).

A likely concern in design is the probability of violating critical limit states which would result in the failure of the subsystem assembly (SSA) which contains the critical component. Although the noncritical failure modes do not directly result in system failure, the degradation caused by their occurrence affects the probability of occurrence of the critical failure modes. Such effects should be accounted for in mechanical system reliability analysis. Therefore, this paper proposes a computational technique to systematically incorporate critical and noncritical failure modes in the estimation of system reliability. The proposed methodology is extended to the problem of risk assessment in a manner that combines the consequence of failure in terms of cost and testing and inspection results. This is shown to result in an efficient reliability-based decision tool to aid in the design and development of structural systems.

The terminology of structural failure and structural design limit states or failure criteria is used for illustration in the current paper. However, the mathematical constructs used to calculate system reliability and system risk are totally generic. The numerical meth-

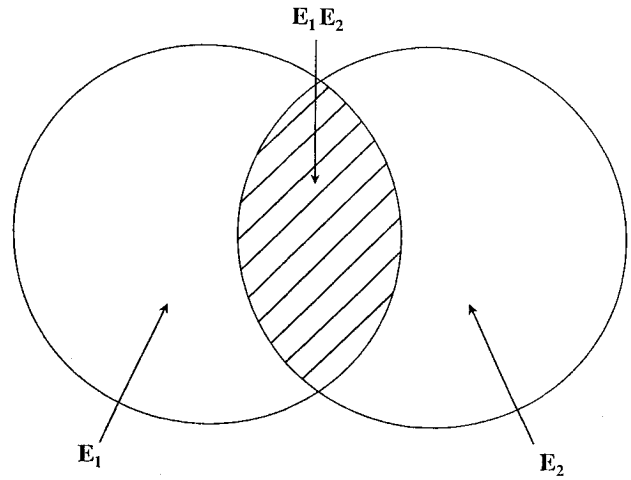

Fig. 1 Venn diagram for simple union.

Received April 15, 1993; revision received Feb. 28, 1994; accepted for publication April 13, 1994.

*Professor, Department of Mechanical Engineering. Fellow AIAA.
†Associate Professor, Department of Civil Engineering.
‡Research Assistant Professor, Department of Mechanical Engineering.
§Graduate Student, Department of Civil Engineering.

ods accept mathematical descriptions of the statistics of the random design variables, as well as the cost functions needed for the risk assessment. Generalized terminology will be used herein to the extent possible, whereas that for structural applications will be used as needed for specificity and clarity.

II. Proposed Methodology

The distinction between critical and noncritical failure modes is maintained in the construction of the failure tree, by identifying several levels. At level I, the probability of each individual failure mode is estimated for an intact system, i.e., no damage has occurred. At level II and above, the probabilities of occurrence of the critical failure modes are estimated after accounting for the noncritical modes. This is done through reanalysis of the system after incorporating the effect of noncritical failure, such as load redistribution and/or changing the finite element mesh to show local cracking.

A. Level I Correlated Events

Consider a system with two critical events E_1 and E_2 at level I. The probability of system failure is the probability of the union of the individual events, which is expressed as

$$P(E_1 \cup E_2) = P(E_1) + P(E_2) - P(E_1E_2) \tag{1}$$

where $P(E_1)$ and $P(E_2)$ are the individual event probabilities, and $P(E_1E_2)$ is the probability of joint occurrence (intersection) of the two events. This is illustrated through the Venn diagram shown in Fig. 1.

The probability of intersection $P(E_1E_2)$ is formally written as

$$P(E_1E_2) = P(E_1 \mid E_2)\, P(E_2) = P(E_2 \mid E_1)\, P(E_1) \tag{2}$$

where $P(E_i \mid E_j)$ is the conditional probability of event E_i, given that event E_j has occurred. If the two events are statistically independent of each other, then $P(E_i \mid E_j) = P(E_i)$ and

$$P(E_1E_2) = P(E_2)\, P(E_1) \tag{3}$$

If the event E_i is fully dependent on event E_j, then $P(E_i \mid E_j) = 1$. If the limit states corresponding to these events share common random variables, then the limit states are correlated and

$$P(E_1E_2) \geq P(E_1)\, P(E_2) \tag{4}$$

The use of Monte Carlo simulation is one option to accurately estimate $P(E_1E_2)$ in the general case of correlated events. However, one may approximate $P(E_1E_2)$ in much the same manner as the first-order reliability method (FORM) approximation to calculate the individual failure event probability $P(E_i)$ (Ref. 2). Let a performance function $g_i(\boldsymbol{x})$ correspond to each failure mode E_i such that $g_i < 0$ indicates the failure event E_i, $g_i > 0$ indicates success, and $g_i = 0$ indicates the limit state. Each performance function is approximated by a linear function as

$$g_i(\boldsymbol{x}) = g_{i0} - \sum_{j=1}^{J} a_{ij}x_j \tag{5}$$

where the linearization of the function $g_i(\boldsymbol{x})$ has been done at the most probable point (MPP) for each of the failure events, and J is the number of randomvariables. The MPP is the set of random variable values that correspond to the most probable condition, at the condition $g_i = 0$ (i.e., on the limit state). In the space of uncorrelated standard normal variables, the MPP is the point on the limit state which has the least distance from the origin,[2] and the minimum distance is referred to as the reliability index and denoted as β. A first-order approximation to the probability of failure is then obtained as $P(g_i < 0) = \Phi(-\beta)$, where Φ is the cumulative distribution function of a standard normal variable.

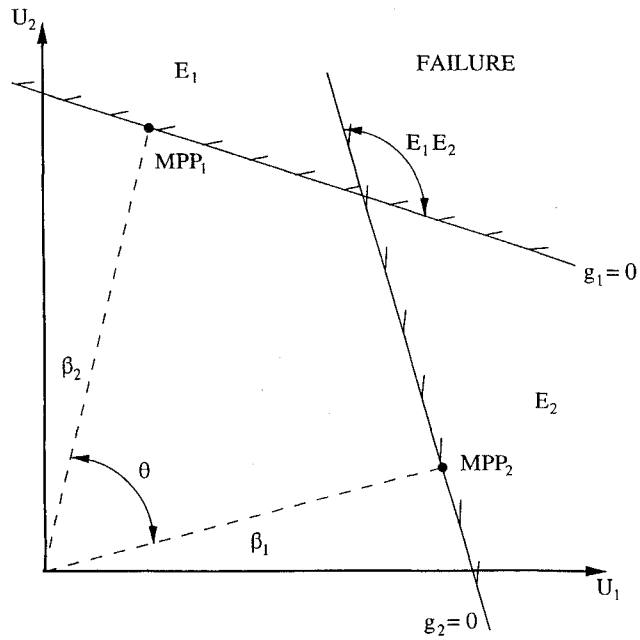

Fig. 2 Intersecting response surfaces.

In two dimensions, Eq. (5) may be illustrated for events E_1 and E_2. The variables have been transformed to uncorrelated standard normal space,[3] and both random variables are assumed to be common to both failure events. The intersection of the two linear surfaces is illustrated in Fig. 2. Additionally, the individual MPPs are shown, along with the reliability indices (β_i) for each event space.

The state probability for the conditional event $\{E_2 \mid (g_1 = 0)\}$ is given by Ditlevsen[4] as $\Phi(-\Delta)$, where Φ is the cumulative distribution function of a standard normal variable, and

$$\Delta = \frac{\beta_2 - \rho\beta_1}{\sqrt{1-\rho^2}} \tag{6}$$

where

$$\rho = \frac{\mathrm{Cov}(g_1, g_2)}{\sigma_1\sigma_2} = \cos\theta \tag{7}$$

is the correlation coefficient between the two linearized limit state functions. Note that $\Phi(-\Delta)$ corresponds only to the probability (for Gaussian distributions) of event E_2, given that event E_1 is *on* the limit state $g_1 = 0$, i.e., $P(E_2 \mid E_1 : [g_1 = 0])$. The joint probability for the intersection space denoted E_2E_1, however, must include all cases $g_1 \leq 0$. For Gaussian distributions, this joint probability can be easily calculated using the bivariate normal integral. This integral uses the information on the individual MPPs and the correlation coefficient ρ between the two linearized limit states in uncorrelated standard normal space. A numerical integration scheme to compute this probability is developed in the Appendix.

B. Sequential Failure Limit Surfaces

The presence of degradation mechanisms in a system results in the redistribution of internal loading, with a consequent change in the probability of failure associated with those critical failure modes linked to the same internal loads. Some examples that are relevant to propulsion system degradation include 1) loss of load carrying capability of a structural member through plasticity or creep, 2) increase in operating temperature due to flow system seal failure, 3) crack growth due to the presence of initiation mechanisms, and 4) disengagement of linked rotor parts due to excessive deflections.

In general, degradation is any state of damage that reduces the functional performance level of any subsystem or component in the system. The degradation mechanisms may be included in the system reliability analysis through the union operation of all level I

events, including both critical and noncritical modes. This approach is seen to produce a conservative estimate of system reliability but does not provide the means for tracking the sequence of failure events from the first level to the final state of system failure. System reliability sensitivity to the primitive random variables is also not accounted for in terms of the flow of influence through the noncritical failure events to the critical failure events.

The multilevel system reliability approach that has been developed in this paper is based on the union of all of the critical failure events. These may take place at level I (intact structure) or at higher levels as the result of any degradation mechanism identified initially at level I. The computational challenge for this problem is to redefine the critical limit states that result from structural system changes brought on by the noncritical, system degradation modes. Specifically, we seek to define the response function for the critical mode that reflects the degradation process. In traditional probability terms, the higher level critical failure event could be seen as the intersection of the critical failure event with the preceding degradation failure mode(s). However, such an intersection operation does not properly account for the physical interaction between the noncritical and critical failure modes; it also results in incorrect sensitivity information. These observations are explained subsequently in mathematical terms.

If the classical probability approach were to be followed without considering the physical effect of noncritical failure, the system failure probability for the multilevel problem will be computed though the union of, say, a level I critical event (E_1^I) with a level II critical event (E_1^{II}), intersected with the level I noncritical event (E_2^I). In this example, we can take the two critical events to be the same failure mode, such that the system failure probability is represented by

$$P_S^{\text{CRIT}} = P[E_1^I \cup (E_1^{II} \cap E_2^I)] \tag{8}$$

Combining the terms in Eq. 8 using standard probability theory, we obtain the final form of the system failure probability for this simple problem

$$P_S^{\text{CRIT}} = P(E_1^I) + P(E_1^{II} \cap E_2^I) - P[E_1^I \cap (E_1^{II} \cap E_2^I)] \tag{9}$$

The resulting system failure probability does not represent the true system state resulting from a degradation process. The intersection process in Eq. (8) does not reflect the internal load redistribution that occurs with progressive damage. Progressive damage is a nonlinear process, requiring an update of the response function defining the event space E_1^{II}, or E_1 updated to the second level. This nonlinear resolution of the response function for E_1 is not the same as an intersection of an event space representing, say, plasticity E_2, with a critical failure mode event E_1. Also, the intersection event cannot be represented by a single response surface; the intersection process results in a joint probability but not a single surface. Therefore accurate sensitivity information regarding the influence of a noncritical mode cannot be obtained with the classical approach, as is possible in the case of single response surfaces.

The answer to the first shortcoming just cited also provides an answer to the second. The approach relies on the previously developed advanced mean value (AMV) method.[5] The progressive damage process for a structural system can be approximated by a sequence of linear response surfaces, each one of which is centered at the MPP for a given level of progressive damage. The sequence is taken in the sense of damage evolution as a sequence of states. The sequential response surfaces define the event space for any nonlinear damage process. At the same time, the critical failure state of the system can be seen as a sequence of response modes, each corresponding to the MPP for a certain level of damage in the nonlinear, progressive damage mode. The nonlinear limit state corresponding to the critical response mode can then be approximated as a sequence of linear limit states. The union of the failure regions defined by these linear limit states then defines the true critical event space E_1^{II}; in that case, no intersection as in Eq. (8) is needed or appropriate. Rather, the sequential limit states capture the physics of the progressive damage process, whereas the classical intersection operation in Eq. (8) merely results in the estimation of the joint probability of two statistically correlated events, without considering the physical effect of progressive damage.

Considering linear limit states in the space of uncorrelated standard normal variables, the linear approximation for the level I noncritical event E_2 is given by

$$D_2(x) = \mu_{2D} + \sum_{i=1}^{J} B_i S_i \tag{10}$$

where D_2 is taken to be the approximation to the design response function, expanded about its mean value μ_{2D} in terms of the standard normal variables S_i given by

$$S_i = (x_i - \mu_i)/\sigma_i \tag{11}$$

(no sum on i), where x_i is the ith random variable, μ_i and σ_i are its mean value and standard deviation, respectively, and J is the number of random variables. Note that if the variable x_i is non-Gaussian, then the equivalent normal mean μ_i^N and the equivalent normal standard deviation σ_i^N (Ref. 2) have to be used in the equation. The resulting response function is called the mean value, first-order response function.[5] The coefficients B_i in Eq. (10) are given by

$$B_i = \frac{\partial D_2}{\partial x_i}\sigma_i|_{\mu_D} \tag{12}$$

As mentioned earlier, the point on the reponse surface which is closest to the origin is called the MPP. The coordinates of the MPP are found, for a linear response surface and Gaussian variables, to be the intersection of the response surface, Eq. (10), and the line whose direction cosines are given by

$$\alpha_i = \frac{\partial D}{\partial x_i}\frac{\sigma_i}{\sigma_D} \tag{13}$$

where σ_i, σ_D are the standard deviation of the independent random variables and the response function, respectively. We denote the MPP by the special variables S_i^*. In the case of linear response functions with Gaussian variables, the probability integral for response conditions exceeding a design limit d_2 is given by the standard Gaussian distribution function Φ as follows.

$$P(D_2 > d_2) = \Phi\left(-\frac{d_2 - \mu_{2D}}{\sqrt{\Sigma B_i^2}}\right) \tag{14}$$

Even for the case of nonlinear response functions with non-Gaussian and correlated variables, well-known transformations to an equivalent space of uncorrelated standard normal variables are available[2] to facilitate the use of Eqs. (10–14).

The advanced mean value algorithm has two key elements. The first element is the resolution of the system response function at the MPP. The updated solution obtained by the resolution assumes that the probability level remains constant, whereas the solution value corresponding to $D_2 - d_2$ changes due to the general fact that the true response function is not a linear function of the design variables. Such updating changes the point corresponding to the condition $D_2 - d_2 = 0$; iteration is performed to satisfy the limit state by a new linear expansion of the response function about the MPP conditions. The new expansion is obtained by new estimates of the first-order derivatives of the response function in terms of the random variables x_i. We shall take the updating step as having been performed. The new response function expansion at the MPP is taken to be given by

$$D_2(x) = d_2 + \sum_i B_i\left(S_i - S_i^*\right) \tag{15}$$

As a first-order approximation, the response function for event E_1 at level II (E_1^{II}) may be expanded at the same MPP for event (E_2^I) with the result

$$D_3(x) = D_{30} + \sum \frac{\partial D_3}{\partial x_i}\sigma_i\left(S_i - S_i^*\right) \tag{16}$$

The probability of the critical mode for Gaussian distributions is then given by

$$P(D_3 > d_3) = \Phi\left[-\frac{d_3 - D_{30} - \Sigma_i\,(\partial D_3/\partial x_i)\,\sigma_i S_i^*}{\sqrt{\Sigma_i\,(\partial D_3/\partial x_i)\,\sigma_i}}\right] \tag{17}$$

The probability in this case includes the effect of event E_2, since the critical failure mode response surface has been redefined corresponding to the progressive damage level at the MPP for event E_2. This first-order approximation is obviously adequate for linear limit states. For nonlinear limit states, an iterative improvement has been suggested by the authors[6,7] to accurately define the sequential limit states.

Another question concerns the number of sequential linear limit states needed to calculate a reasonable estimate of the system reliability. If the progressive damage state increment is small, the new surface for the critical event will be highly correlated with the previous response surface for the same critical event; the resulting high degree of correlation means that the system reliability does not change very much. Larger progressive damage steps result in greater changes to the system reliability but may introduce greater errors. An adaptive scheme to address this question is described in Ref. 8.

The reference to progressive damage here does not directly incorporate time-dependent reliability computations which involve random process modeling of loads and resistances. The emphasis is on updating the system limit states for different levels of accumulated damage.

C. Sequential Failure Probability

The preceding two subsections dealt with 1) the calculation of the joint probability of two correlated events, and 2) the definition of a new response surface for a critical event which is modified by a preceding noncritical event. The new response surface is obtained as a set of multiple linear response surfaces corresponding to different levels of progressive damage. The current subsection considers the use of the results of 1) and 2) in the final calculation of bounds on system reliability.

Two kinds of level I noncritical events are identified in Fig. 5. The first is progressive damage, such as violating the structural yield limit condition. This damage can be treated as a sequence of states involving greater and greater amounts of degradation, without catastrophic system failure. Generally then, yield is a progressive damage mode, requiring (possibly) multiple new "subsequent" response surfaces, each one of which may be denoted $g_i|_j$.

The second kind of subsequent event is illustrated by a structural example, as in the disengagement of a spacer from a rotor assembly. In this case, there is an engagement (state 1) and a disengagement (state 2) condition of the rotor. The natural frequencies of vibration for the two states are different due to the presence or absence of the stiffening effect of the spacer. For such binary noncritical failures, there is only one subsequent response surface. Binary failure conditions are exclusive events in probability terms, and result in certain simplifications for system reliability calculations. In what follows, both cases are considered in terms of a single subsequent failure event; the generalization to multiple surfaces is straightforward.

For a progressive failure mode, such as rotor burst after yielding of the ring, the total probability of rotor burst is made up of the union of a sequence of subsequent critical events denoted as burst/yield (i.e., rotor burst, given the yielding of the ring). If Δ_1, Δ_2, etc., correspond to increasing amounts of yield, the probability of rotor burst may be written as

$$P(\text{burst}) = P(\text{burst} \mid \text{no yield} \cup \text{burst} \mid \Delta_1 \text{ yield} \cup \text{burst} \mid \Delta_2 \text{ yield} \cup \ldots) \tag{18}$$

For each state in Eq. (18) there is a response surface which is defined at a given amount of yield.

The union of these surfaces in Eq. (18) will reflect the fact that each response state will be highly (but not totally) correlated with the previous response state. Therefore, only a few progressive damage levels may need to be included to compute the probability in Eq. (18). Thus, for any progressive damage problem, the final critical failure event space and the corresponding probability could be approximated through a relatively coarse sequence of intermediate states. In some problems, it may be adequate to reduce the sequence to two states, with the first state corresponding to an intact system and the second state corresponding to a high degree of degradation associated with the noncritical failure mode.

The first step in generating a subsequent response surface is the reanalysis of the structure. The first-order approach presented in this paper performs this reanalysis at the MPP associated with the current level of progressive damage. The imposition of the MPP condition for such reanalysis might be the extension of plasticity up to a certain node or the simulation of a certain amount of crack growth.

The second step is to generate the performance function for the critical limit state at this MPP, as given for the simple problem in Eq. (16). The performance function is referred to as g_i^Λ to denote that it is the ith failure mode being incurred at the Λth response level (> 1). The response surface so generated reflects the effect of the degraded state in its evaluation. However, if the perturbations used to define the response surface are not consistent with the intended degraded condition (e.g., elastic unload from a plastic condition), then the slope of the response function will be that associated with the undegraded response. Therefore, for the greatest accuracy in getting the subsequent response function, it is recommended that the perturbations be as consistent with increasing degradation as possible.

D. System Reliability Bounds

The system reliability strategy is to recognize that each higher level response surface basically defines another part of the system failure domain. Therefore the probability of failure is simply the probability of union of failure regions defined by all of the response surfaces for the critical failure modes. The expression for the probability of union of all of the critical events is expanded as in Eq. (19). Letting E_i be the event space for any level I critical event, and $E_{i|j}$ be the subsequent event space for the ith critical failure mode, we obtain

$$P_S^{\text{CRIT}} = P(E_1) + P(E_2) + \cdots + P(E_{i|j}) + \cdots - P(E_1E_2) - \cdots - P(E_1E_{i|j}) + P(E_1E_2E_3) \cdots + P(E_1E_2E_{i|j}) + \cdots \tag{19}$$

showing the intersection probabilities up through the three-event intersections.

A first-order multinormal integral approximation is available to estimate the intersection probabilities of more than two events.[9] Alternatively, second-order bounds for P_S^{CRIT} may be used in which only two-event intersection probabilities are calculated. It should be noted that such bounding is only valid in the case of linear response functions and Gaussian distributions and therefore will not be strictly true for the nonlinear problem. However, to best approximate P_S^{CRIT} in Eq. (19), we keep the linear bounding notation in what follows.

The complement of the union of all complementary critical events in Eq. (19) is used to write the critical failure probability as

$$P_S^{\text{CRIT}} = P\left(\cup_{i=1}^n E_i\right) = P\left(\overline{\cap_{i=1}^n \bar{E}_i}\right) = 1 - P\left(\cap_{i=1}^n \bar{E}_i\right) \tag{20}$$

where $\bar{E}$ is the complement of E, and

$$P(E) = 1 - P(\bar{E}) \tag{21}$$

The lower bound of $P\left(\cap_{i=1}^{n}\overline{E}_i\right)$ provides an upper bound to Eq. (20). Combined with the second-order result, the following upper bound is suggested:

$$P_S^{\text{CRIT}} = P\left(\cup_{i=1}^{n}E_i\right) \le \left\{\sum_{i=1}^{n}P(E_i) - \max\left[\sum_{i=2}^{n}\max_{j<i}P(E_iE_j),\ \max_{1\le i\le n}\sum_{j=1,j\ne i}^{n}P(E_iE_j)\right]\right\} \quad (22)$$

The lower bound of the critical system failure probability is less important than the upper bound, which sets the minimum system reliability for a linear system. However, to get a sense of the sensitivity of the system reliability to the correlations of the individual modes, the lower bound of the system failure probability is given as

$$P_S^{\text{CRIT}} = P\left(\cup_{i=1}^{n}E_i\right) \ge \max_{1\le j\le n}\left\{P(E_j) + \sum_{i=1,i\ne j}^{n}\max\left[\left(P(E_i) - \sum_{k=1,k\ne i}^{\max(i,j)}P(E_iE_k)\right);0\right]\right\} \quad (23)$$

A summary of several forms of the upper and lower bounds including the derivation of the upper and lower bounds in Eqs. (22) and (23) is given in Ref. 11. The second-order bounds widely used in the literature provide the narrowest bounds if the failure events are arranged in the descending order of failure probability; the bounds suggested here remove this restriction by computing all of the two-event intersection probabilities.

The upper and lower bounds in Eqs. (22) and (23) include the correlated two-event probabilities calculated from the failure event tree for all critical events, at any level. It is expected that the bounds will be reasonably close to each other, as the joint probability of three or more events is likely to be small. Experience will have to confirm this expectation.

E. System Reliability Sensitivity Factors

The probabilistic sensitivity factors for an individual limit state are given by the direction cosines of the vector from the origin to the MPP. No such single vector describes the system failure state, because the system failure probability is being computed as the probability of union of the individual failure events. The probabilistic sensitivity factors are effective in determining which random variables are most important in affecting the design reliability. The sensitivity factors of individual limit states may be combined to derive first-order system sensitivity factors which contain information on the physical sensitivities as well as the stochastic variabilities, in the following manner.

The vector to the individual event (denoted by i) most probable points $(\text{MPP})_i$ is defined with length β_i and direction cosines which are the probabilistic sensitivity factors α_{ij}. The subscript j refers to the random variable. The sensitivity factors combine the local physical sensitivities $\partial g/\partial x_j$, as well as the standard deviation σ_j of each random variable. If some of the random variables are nonnormal, then the equivalent normal standard deviation σ_j^N should be used.

Now define a probability-weighted system sensitivity vector that combines the individual failure-MPP location vectors in the standard normal space as

$$\phi_j = \sum_{i=1}^{N}\alpha_{ij}P(E_i) \quad (24)$$

where N is the number of limit states. The system failure vector is then taken to be the vector $\vec{\Phi}$, given as

$$\vec{\Phi} = \sum_{j=1}^{NRV}\phi_j e_j \quad (25)$$

where e_j are the unit basis vectors in standard normal variable space. The resulting system vector direction cosines are proposed as system reliability sensitivity factors. These factors reflect the combination of dominant random variables through the direction cosines to each MPP (α_{ij}), and the dominant failure modes through the individual event probabilities $P(E_i)$.

III. System Risk Assessment

Risk is measured here in terms of the monetary consequence of failure. Therefore, system risk assessment is taken to be the computation of the expected cost of a critical system failure event, i.e., the product of the probability of the event times the cost consequence of the event. The consequences of component failure within a system context are likely to be complicated trees with branches representing various failure scenarios. Probabilities can be assigned then to individual branches in the consequences tree to reflect likely failure scenarios. Costs are then assigned to critical locations on the event consequences tree.

One element in planning scenarios on a failure consequences tree is the presence of inspections or failure detection systems. The presence of instrumentation in testing complicated systems is provided to document failure data in real time, as well as to provide advance warning, hopefully of noncritical damage or degradation behavior in the system that will allow for noncatastrophic system shutdown. The cost of providing the instrumentation or inspections and the probability of success of the instrumentation or inspections combine to determine the expected reduction of risk (cost) of a catastrophic event. Thus, the linkage of system reliability prediction with such a failure consequences tree can provide realistic trades between inspection cost and risk of failure. The event tree must define the probability that the failure—if it occurs—will occur in a particular mode such as a component test, a subsystem assembly (SSA) test, full-scale system acceptance testing, and actual system operations. The event tree must also show the consequences of failure detection. A detected critical state precludes the occurrence of the next event in the tree, but requires corrective action, such as SSA replacement. Thus, failure detection has cost, but the cost is less than that for an undetected event.

The probability of damage detection differs for each mode of degradation or failure. Furthermore, the probability of detection differs between the different levels of testing/operation. For example, damage detection is more likely in a component test than in an SSA test; failure detection is more likely in SSA testing than in full system acceptance testing, and so on. The proposed approach is to define the total probability of detection as the product of the probability based on a testing level, and the probability for the given mode of damage. Relatively arbitrary initial levels of probability have been selected for an example problem but can be easily modified by the code user.

A simple example of a failure event consequences tree for critical and noncritical degradation failure modes in a space propulsion system has been proposed as shown in Fig. 3. Since each system is unique, it is difficult to formulate a generic failure consequences tree for all systems. The methodology has been illustrated herein using a simplified view of the failure of a critical element in a space propulsion system similar to the National Space Transportation System (Space Shuttle). The consequences tree for such a problem, shown in Fig. 3, indicates the probabilities of detection (POD1, POD2, etc.) of failure at various levels, and the associated costs of failure (C1, C2, etc.). The event consequences end with cost functions, which the user can supply. No added risk due to inspection instrumentation has been included in the present failure consequences tree. Furthermore, the illustrated tree does not account for the cost/benefit factors of component refurbishment. However, the proposed idea of including a consequences tree in risk assessment is rather general, and the tree can be modified to account for these additional conditions.

The computation of system risk as the expected cost of system failure involves the cost of union of several critical failure modes. Consider two critical failure modes E_1 and E_3. Since the cost of joint occurrence of the two failure modes is unavailable, the ex-

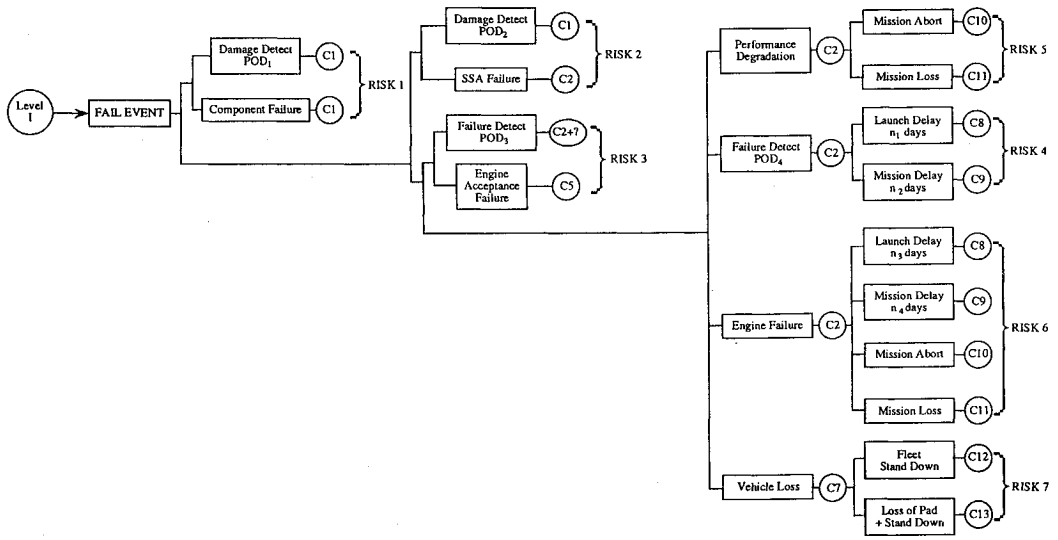

Fig. 3 Failure event consequences tree.

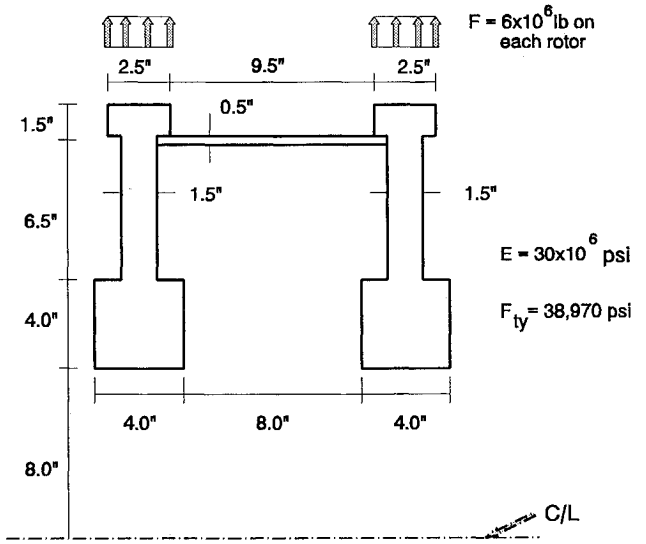

Fig. 4 Simplified rotor model.

pected cost of the union may only be expressed in terms of bounds, as

$$C(E_1 \cup E_3) \geq C_1 P(E_1) + C_3 P(E_3) - \max(C_1, C_3) P(E_1 E_2)\mu \quad (26)$$

and

$$C(E_1 \cup E_3) \leq C_1 P(E_1) + C_3 P(E_3) + \min(C_1, C_3) P(E_1 E_2) \quad (27)$$

Thus, even for a system with only two failure modes, the expected cost of system failure can only be bounded. Therefore, the risk assessment result for a complex system will be less accurate than the system reliability result. Nevertheless, the risk result still provides a useful decision tool in assessing the cost vs benefit trades for different reliability enhancement strategies.

IV. Numerical Example

A. Problem Description

The system reliability and risk assessment methodology proposed in the preceding sections is illustrated by application to the simplified rotor system shown in Fig. 4. The methodology has been implemented in the numerical evaluation of stochastic structures under stress (NESSUS) computer code,[1] developed through the probabilistic structural analysis methods (PSAM) program under the leadership of NASA Lewis Research Center. The rotor system consists of two disks, an interference-fit spacer, and dummy blade masses. The rotor operating environment is modeled with a random rotor rotational velocity and random temperatures. The interference fit between the rotor and the spacer is taken to be random, i.e., the length of the gap between the spacer and the disk is a random variable, with a mean value equal to zero. Nonnegative interference is taken to be needed for the modal vibration of the entire assembly, rather than of the disk alone.

Table 1 Random variable definitions

Variable	Mean	Standard dev	Distribution
E_{Rotor}, msi	20	0.40	Lognormal
E_{Ring}, msi	17	0.34	Lognormal
ρ_{Rotor}, lb/cu.in.	0.0008	0.000016	Lognormal
ρ_{Ring}, lb/cu.in.	0.0008	0.000016	Lognormal
F^{tu}_0, ksi	123	12.3	Lognormal
F_{ty}, ksi	96	9.6	Lognormal
A_{LCF}	2.2*E*10	2.2*E*9	Lognormal
b, in.	4	0.0	Deterministic
K_{IC}, ksi $\sqrt{\text{in.}}$	50	5	Lognormal
a_i	0.002	0.0002	Weibull
C	1.45*E*-9	1.45*E*-10	Lognormal
n	2.61	0.0	Deterministic
δ_{INT}, in.	0.0	0.05	Normal
ΔT, °F	0	53	Extreme value
Ω, rad/s	628	49	Extreme value

The strength or resistance models used in the analysis are now discussed. In the case of the current example, the burst condition is taken to occur when the average hoop stress exceeds a shape factor times the material ultimate strength; the same approach is used for yield of the spacer ring. The crack initiation life (N_{LCF}) is computed through a simple power law model, given as

$$\Delta N = A\Delta\varepsilon^{-b} \quad (28)$$

The parameters A and b are defined in Table 1, where b is taken to be deterministic. The number of cycles of crack propagation to fracture N_{FM} is also computed using a simple Paris law relation

$$\Delta N_{\text{FM}} = C\Delta K^n \quad (29)$$

where C and n are also defined in Table1, and where n is also taken to be deterministic.[10] The total fracture mechanics life is computed for two locations differently, to illustrate two types of situations. In the bore region of the disk, the fracture mechanics life is the life from an initial defect size a_i, whereas in the rim region the crack is initiated to a size of 0.030 in. according to the crack initiation model given in Eq. (28). Finally, the deterministic target life for both fracture mechanics limits is taken to be 10,000 cycles. Fracture prior to this limit is taken to be a critical failure mode.

The high-cycle fatigue mode of component failure in the example is taken to occur if any of the system natural frequencies falls within a specified range of a fixed cyclic frequency. Resonance

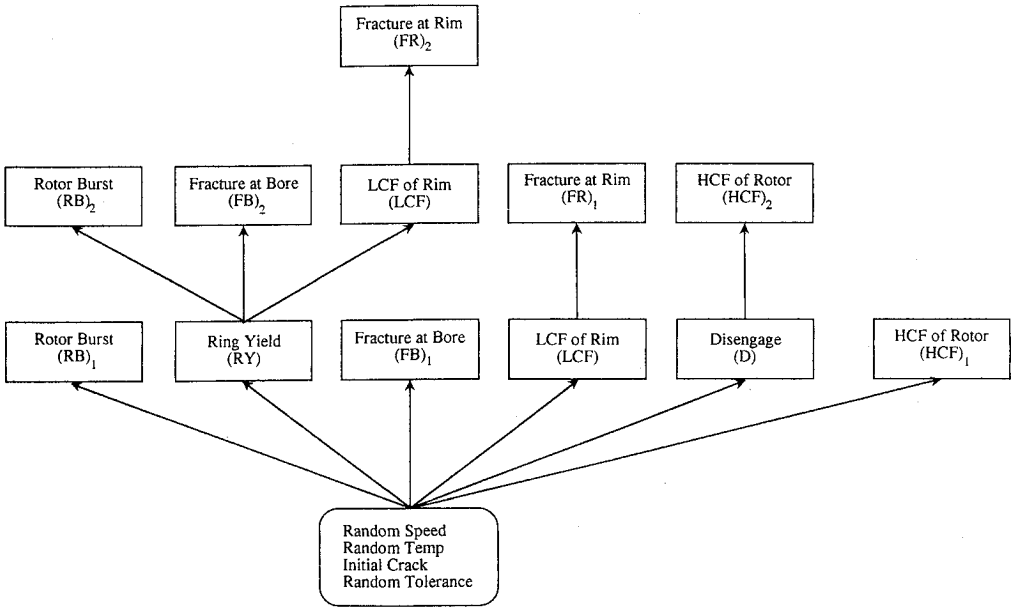

Fig. 5 Example failure mode scenarios.

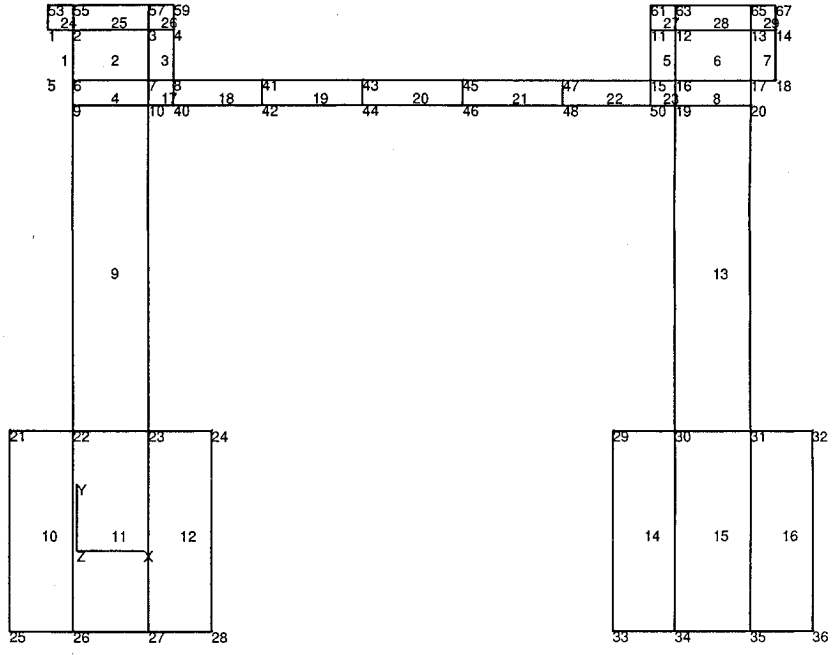

Fig. 6 Coarse finite element model of rotor.

can occur in the system if any of the system natural frequencies falls within the range of interest. The probability of resonance would be different for different natural frequencies. The overall probability of resonance reduces to the sum of the probabilities of resonance from individual frequencies, since these are mutually exclusive conditions. The probability of resonance would be the greatest for the natural frequency that is closest to the range of interest, and the probability can be expected to rapidly diminish for natural frequencies away from this range, so that it should be adequate to consider only very few natural frequencies. In this numerical example, the first frequency is observed to give the highest probability, and the contributions of the other frequencies are negligible. The structure is assumed to have negligible damping, since the inclusion of damping will make the model complicated. The purpose here is to illustrate the type of event that follows a binary event state for the structure—an engaged spacer which acts to stiffen the system and a disengaged spacer. Other binary failure states in turbomachinery include dampers that work or not and heat pipes that work or not.

The critical design limit states considered in the example are rotor burst, due to the average hoop stress exceeding the shape-dependent ultimate strength of the rotor (*RB*), fracture of the bore due to fatigue crack growth from an intrinsic defect of size a_i (*FB*), fracture at the rim due to crack initiation (*FR*), and fracture of the rotor due to high-cycle fatigue (HCF). Therefore, system failure can occur in this example if any of these limit states is violated.

The critical limit states can be violated with and without load redistribution in the rotor system due to noncritical damage. The noncritical damage modes considered in this example are 1) progressive yielding of the spacer and 2) disengagement of the spacer

and one of the disks. These critical limit states and progressive damage modes are illustrated in Fig. 5. The critical limit states can be violated at level I (no load redistribution due to any damage; the structure is intact), or at a higher level (after noncritical damage). System probability of failure is then computed as the probability of union of the critical events,

$$P_S^{\text{CRIT}} = P(RB^I \cup FB^I \cup FR^I \cup \text{HCF}^I \cup RB^{II} \cup FB^{II} \cup FR^{II} \cup \text{HCF}^{II})\text{x} \tag{30}$$

which may be written symbolically for the general, multilevel failure problem as follows:

$$P_S^{\text{CRIT}} = P\left(E_1^I \cup E_2^I \cup \ldots \cup E_1^{II} \cup \ldots\right) \tag{31}$$

All of the limit states are first approximated through linear functions using the first-order reliability approach. A mean value, first order (MVFO) estimate of the probability distribution is computed for a given limit state.[5] The MVFO solution can also be used as the basis for an improved solution through a simple updating procedure at each user-defined reliability level, known as the AMV. The MVFO or AMV options give the individual probability levels for each event, along with the response surface data. Each failure event is represented through a limit state $g_i^{\Lambda}(x) = 0$, where i denotes the event and Λ defines the level. The probability distribution for the response function is calculated by the fast probability integration algorithm.[3]

All events on level I are denoted initial failure modes (IFM). The IFMs are generally dependent on the basic random variables, which may be common for several IFMs (e.g., rotor speed), or uniquely related to only one IFM (e.g., ultimate tensile strength). The presence of common random variables means that the limit states for the failure events are correlated. System reliability calculations take explicit account of this correlation, as has been shown in the preceding sections.

The structural system is modeled for the sake of illustration using a coarse finite element mesh with 23 four-node axisymmetric elements. In addition, eight elements with very small stiffness are used to represent the mass of the blades. The connectivity is shown in Fig. 6.

The parameters of the random variable distributions are selected as shown in Table 1. The values do not reflect any real design and are only used for the sake of illustration but are selected in a way to produce system response with realistic design limit state simulation. Most of the variables in Table 1 are assumed to have a log-normal distribution, except a_i, ΔT, and Ω. The operating speed Ω and the operating temperature ΔT are similar to load variables. In general, the load variables have been used with an extreme value distribution in reliability analysis; therefore, both the variables are assumed to have an extreme value distribution. The initial defect size a_i is assumed to have a Weibull distribution for the sake of illustration. However, the proposed methodology is not restricted to the use of these distributions.

B. First Level Failure Events

The structural system is analyzed for the following failure modes.

1. Rotor Burst

If the average hoop stress exceeds the tensile strength of the rotor, the rotor is assumed to have failed by bursting. Temperature affects both S and R, since the bursting strength reduces as the temperature increases. This strength degradation is simulated using a generic multifactor interaction (MFI) model by which the mean value of the ultimate strength is reduced. The MFI equation used is

$$\bar{F}_{tu} = \bar{F}_{tu}^0 \left(\frac{TT_F - TT}{TT_F - TT_0}\right)^Q \tag{32}$$

where $\bar{F}_{tu}^0$ is the mean value of the bursting strength at temperature TT, $\bar{F}_{tu}$ is the mean value of the bursting strength at temperature TT_0, and TT_F is the temperature at zero strength. $\bar{F}_{tu}^0$ is given in Table 1. The values assumed for the other parameters are:

$$Q = 0.5 \qquad TT_0 = 0 \qquad TT_F = 270 \tag{33}$$

Note that the value of TT_F is derived using following data: 100-deg overtemperature produces 20% reduction in strength and 200-deg overtemperature produces 50% reduction in strength.

The probability of failure by rotor bursting is $P(E_1) = 0.0008937$.

2. Ring Yield

This is a nondestructive limit state in which the stress at node 42 in the ring is checked for yielding. Use of this node indicates significant but not final levels of plasticity. The yield stress is taken to be a random variable. The limit state is a simple excedance condition on stress, using yield stress.

The probability of failure by ring yield is $P(E_2) = 0.019590$.

3. Fracture Crack Growth at Inner Bore

This is a critical limit state in which failure is assumed to occur if the rotor fails by fracture crack growth during the service life of the system (assumed to be 10,000 cycles). The Paris law model described in Eq. (29) is used, and the performance function is written as $g = 10{,}000 - N_{FM}$. The stress variation in each cycle is from 0 to 100%. The crack growth exponent is taken to be deterministic (2.61) and the stress concentration factor is also taken to be deterministic (1.0). The stress at the inner bore is evaluated by taking an average of the stresses at nodes 25–28, shown in the finite element mesh in Fig. 6.

The probability of failure is computed to be 0.1722 if the crack exists. The probability of such a crack occurring is arbitrarily taken to be 0.01, and the resulting probability of failure due to fracture mechanics of a buried crack is found to be $P(E_3) = 0.001722$.

4. Crack Growth from Rim Crack Initiation

This limit state checks the combined life of crack initiation due to low-cycle fatigue (LCF) followed by failure due to crack growth at the external rim of the rotor. The stress at the rim is computed with a random stress concentration factor of $K_t = 2.5$ with a standard deviation of 0.125. The crack growth parameters are the same as those used earlier. The LCF and fracture equations are programmed as part of the user-defined limit state function. The stress at the rim is evaluated by taking an average of the stresses at nodes 1–4. The probability of failure is $P(E_4) = 0.00000171$.

5. Disengagement of the Spacer Due to a Misfit

If the diameter of the spacer ring is smaller than the inner diameter of the rim, the ring may be disengaged during the operation. This is a noncritical failure, but a disengaged rotor will have lower natural frequencies. The lower natural frequencies may resonate during normal operation and that may lead to failure by HCF. Since there are no gap elements in NESSUS, this error or tolerance is simulated by applying a temperature field on the ring alone. The disengagement is assumed to occur when the stress at node 8 or 39 is tensile.

The probability of failure in disengagement is $P(E_5) = 0.002469$.

C. First Level System Reliability m

The first level system reliability may be evaluated either by taking a union of all of the events at the first level or the union of just the critical events. These two forms are written as

$$p_{f_1} = P(E1 \cup E2 \cup E3 \cup E4 \cup E5) \tag{34}$$

$$p_{f_2} = P(E1 \cup E3 \cup E4) \tag{35}$$

The limit states are partially correlated with each other because they share some basic random variables. As mentioned earlier, due to the difficulty in accurately evaluating the joint probabilities of

Table 2 Sensitivity factors of first level events

Variable	Bursting	Ring yield	Fracture	LCF	Disengage
E_{Rotor}	0.000319	0.006549	0.001200	0.002859	0.057007
E_{Ring}	0.000374	0.062508	0.001287	0.002731	0.057608
Rotor density	0.029184	0.007767	0.043840	0.033194	0.022207
Ring density	0.001148	0.049395	0.002665	0.003583	0.085520
Speed	0.361169	0.956119	0.993653	0.994096	0.305395
Temperature	0.923683	0.075660	0.006793	0.019855	0.147723
F_{tu}	0.124553				
F_{ty}		0.271405			
K_{IC}			0.030844	0.014726	
a_i			0.034005	0.017104	
C			0.092562	0.048691	
K_t					
A_{LCF}				0.085162	
Ring tolerance				0.010723	0.933025

Table 3 Sensitivity factors for second level events

	Bursting	Fracture	LCF	HCF
E_{Rotor}	0.030643	0.128183	0.001834	0.404169
E_{Ring}	0.006499	0.024999	0.019750	
Rotor density	0.042046	0.129572	0.070662	0.914684
Ring density	0.013327	0.016507	0.022007	
Speed	0.175988	0.784259	0.958234	
Temperature	0.025519	0.118549	0.030338	
F_{tu}	0.960440	0.022095	0.004665	
F_{ty}	0.207376			
K_{IC}		0.191653	0.054079	
a_i		0.200904	0.131111	
C		0.509102		
K_t			0.226638	
A_{LCF}			0.022314	
Ring tolerance				

Table 4 Sensitivity factors for two failure scenarios

Name	p_{f_1}	p_{f_2}
E_{Rotor}	−0.0014157	0.0014394
E_{Ring}	0.0642958	−0.0015522
Rotor density	0.0189261	0.0569104
Ring density	0.0340583	0.0033047
Speed	0.8042535	0.9140078
Temperature	0.5131453	0.3825665
F_{tu}	−0.0045454	−0.0291754
F_{ty}	−0.2615360	0.0
K_t	0.0000227	0.0001456
A_{LCF}	−0.0000028	−0.0000182
K_{IC}	−0.0055003	−0.0353047
a_i	0.0060382	0.0387575
C	0.0166208	0.1066841
Tolerance	−0.1242557	0.0

three or more events, the system probability of failure is computed using second-order bounds, as follows.

$$0.01499486 \le p_{f_1} \le 0.01500519 \tag{36}$$

$$0.002541011 \le p_{f_2} \le 0.002541013 \tag{37}$$

The second-order lower and upper bounds are seen to be very close to each other for this problem. In other words, the joint probabilities of three or more events seem to be negligible.

D. First Level System Sensitivity Factors

The first level system sensitivity factors are computed from the sensitivities for each individual limit state using Eqs. (24) and (25). The sensitivity factors for all first level events are shown in Table 2. These sensitivity factors indicate the relative importance of different variables in affecting the individual critical failure modes, without considering the effect of noncritical damage, such as yielding of the ring. When the noncritical damage is considered, the sensitivity factors are changed to the values shown in Table 3. The sensitivity factors help the designer in making redesign decisions to satisfy the target reliability.

The system sensitivity factors for p_{f_1} and p_{f_2} are shown in Table 4 by the name used for each independent random variable.

E. Second Level Failure Events

The second level analysis is performed by reanalyzing the structure at the most probable point of the corresponding noncritical event. (As mentioned earlier, this is a first-order approximation; a refined approach for nonlinear limit states is discussed by the authors in Ref. 7.) The same critical limit states are evaluated for the system condition under the noncritical damage. The second-level failure events and their probabilities are found to be rotor burst, probability of failure is $P(E_6) = 0.002620$; fracture at bore, probability of failure is $P(E_7) = 0.0067467$, and LCF leading to fracture at rim, probability of failure is $P(E_8) = 0.0044017$. For the HCF of the rotor, the disk is analyzed for eigenvalues as a free-free structure. Failure occurs if the natural frequency is within a margin of the specified limit. The probability of failure is $P(E_9) = 0.0071623$.

The system probability of failure is computed using

$$p_{f_3} = P(E1 \cup E3 \cup E4 \cup E6 \cup E7 \cup E8 \cup E9) \tag{38}$$

The bounds on the probability of failure are computed to be

$$0.0173408 \le p_{f_3} \le 0.0190313 \tag{39}$$

From the bounds we see that the reliability of the system is predicted to be greater than 0.98097. From the first-level analysis, the critical event reliability was about 0.99745, whereas the reliability including both critical and noncritical events was 0.98499. For this problem, the higher level events were so strongly correlated with the first-level noncritical events that the system reliability result did not change very much as we went from one level to another. It is not likely that this result will hold for all cases. The most critical observation to make is that the system reliability predictions at level I are unconservative, relative to the value predicted by the new system reliability algorithm.

The results of the proposed methodology have been verified with Monte Carlo simulation for simpler problems such as a three-bar truss, a thick cylinder, etc.[11] For such problems, the structural analysis is very simple; therefore, Monte Carlo simulation is not expensive. However, for the present rotor problem, where each structural analysis requires a considerable amount of computation, the strategy of verification with simulation becomes prohibitively expensive. In fact, it is due to the expensiveness of the simulation techniques that the sensitivity-based methods such as the one in this paper are developed for the reliability analysis of practical problems. Advanced sampling techniques to improve the efficiency of simulation are available.[12] These are currently being applied to simpler problems with closed-form performance functions and need to be combined with finite element analysis for larger problems.

F. Second Level System Sensitivity Factors

The sensitivity factors of various second level events are summarized in Table 3. These sensitivity factors correspond to those

for the individual events listed in the headings of the table. Comparison with first-level sensitivity factors in Table 2 shows the effect of ring yield on the various system failure modes. Tables 2 and 3 can be used together by the designer to make decisions regarding the variables to change to meet the reliability criteria.

The system sensitivity factors are computed using Eqs. (24) and Eq. (25). The results are summarized in Table 5.

G. System Risk Assessment Results

The failure consequences tree of Fig. 3 is used for system risk assessment. The probabilities of detection (POD) and the costs of failure (C) for the example problem are chosen as shown in Tables 6 and 7, respectively. The values chosen are only for the sake of illustration.

The total risk computed for the rotor system in this example, using the consequences tree, the probabilities of failure and detection, and the associated costs are

$$\$503{,}000 \leq \text{cost} \leq \$683{,}000 \tag{40}$$

A more important result is the sensitivity of risk to management decisions regarding the investment of finances at different stages of design, testing, and development of the system. The effect of the decision is modeled in terms of changes in the input data. For example, the investment may be such that there is a technology improvement that improves the probability of detection by 10% at the component test level (i.e., the value of POD1 now becomes 0.99 in Table 6). This leads to the reduction of risk, and the benefit is computed to be

$$\$117{,}000 \leq \text{benefit} \leq \$159{,}000 \tag{41}$$

On the other hand, if the investment is toward improvement in POD at the subsystem assembly testing by 10% (i.e., the value of POD4 now becomes 0.11 in Table 6), then the benefit is computed to be

$$\$16{,}000 \leq \text{benefit} \leq \$22{,}000 \tag{42}$$

The results are logical, since improved detection of failure at an early stage is expected to result in larger benefit.

Table 5 Sensitivities for p_{f_3}

Name	In $u(i)$ space
E_{Rotor}	0.224676
E_{Ring}	−0.018700
Rotor	0.507893
Ring	−0.015600
Speed	0.737206
Temperature	0.166526
F_{tu}	−0.020743
F_{ty}	0.089632
K_{IC}	−0.112593
a_i	0.109672
C	0.264843
K_t	0.077381
A_{LCF}	−0.007667
Tolerance	0.0

Table 6 Probabilities of detection

Failure event	POD
Plasticity	0.10
Fracture	0.10
Burst	0.01
HCF	0.10
POD1	0.90
POD2	0.75
POD3	0.30
POD4	0.10

Table 7 Costs of failure

Cost item	Cost, $
C1	50,000
C2	2×10^6
C5	65×10^6
C6	35×10^6
C7	2×10^9
C8	1.44×10^6
C9	240,000
C10	35×10^6
C11	250×10^6
C12	4×10^9
C13	6×10^9

V. Conclusion

A methodology for system reliability and risk assessment has been formulated in this paper and has been demonstrated for application to propulsion structures. The failure modes are divided into two categories, critical and noncritical, and the system failure probability is computed through the union of critical failure events. The effect of noncritical damage on the critical failure events is computed through reanalysis after imposing the noncritical damage. The resulting multilevel representation of system failure is seen to provide a physically meaningful use of the probability computation.

Another important advantage of the proposed method is the computation and use of sensitivity information not only at the level of individual component reliability but also at the level of system reliability and system risk. The multilevel representation provides a means to quantify the effect of progressive damage on different system critical modes, and the use of the limit state methodology preserves the sensitivity information throughout all of the steps of the analysis. The probabilistic sensitivity factors combine the information on both the structural response sensitivity to, and the statistical variation of, the primitive random variables. This is perhaps the most useful outcome of this methodology for the designer, since it helps in rational design and investment decisions to meet the required reliability goal.

The proposed system risk assessment method measures the expected cost of system failure and includes the probabilities of detection and the cost associated with failure through a consequences tree. The consequences tree is seen to properly account for different stages in the development of the system. The resulting cost-benefit calculations help to provide a management decision orientation to reliability analysis.

Appendix: Joint Probability of Two Events

The calculation of the joint probability for two events with known linear response surfaces begins by representing the response surfaces in terms of the standard normal variables corresponding to each basic random variable. The representation is given by the n-dimensional hyperplanes

$$g_1 = a_0 + \sum_{i=1}^{n} a_i u_i \tag{A1}$$

$$g_2 = b_0 + \sum_{i=1}^{n} b_i u_i \tag{A2}$$

where u_i is the standard normal random variable corresponding to the physical random variable x_i with mean value μ_i and standard deviation σ_i

$$u_i = (X_i - \mu_i)/\sigma_i \tag{A3}$$

The calculation of the joint probability is developed herein using the Ditlevsen construction, which is illustrated in Fig. 2 for two correlated limit states with two uncorrelated random variables. The reliability indices for the limit states $g_i(x_1, x_2) = 0$, $(i = 1 \text{ or } 2)$ are given in terms of the distances from the origin β_{10} and β_{20}. The reliability indices correspond to the number of standard deviations for each limit state, such that the $P(g_i \leq 0) = \Phi(-\beta_i)$, where Φ is the standard Gaussian distribution function. Thus, the β corre-

spond to probability levels for various levels of the response surfaces.

The correlation coefficient ρ for two partially correlated limit states is given by

$$\rho = \sum_{i=1}^{n} (a_i b_i) \Big/ \sqrt{\sum_{i=1}^{n} a_i^2 \sum_{i=1}^{n} b_i^2} \tag{A4}$$

The joint probability density function for two normally distributed, partially correlated random variables is then written as

$$f(g_1, g_2) = \frac{1}{2\pi\sqrt{1-\rho^2}} \exp\left[-\frac{1}{2(1-\rho^2)}\left(\beta_1^2 - 2\rho\beta_1\beta_2 + \beta_2^2\right)\right]$$

$$= \frac{1}{\sqrt{2\pi}} \exp\left(-\frac{1}{2}\beta_1^2\right) \frac{1}{\sqrt{2\pi}\sqrt{1-\rho^2}} \exp\left[-\frac{1}{2}\left(\frac{\beta^2 - \rho\beta_1}{\sqrt{1-\rho^2}}\right)^2\right] \tag{A5}$$

The joint probability $P(E_1 E_2)$ is then calculated as the integral of the joint density function over the joint area A as

$$P(E_1E_2) = \int\int \frac{1}{\sqrt{2\pi}} \exp\left(-\frac{1}{2}\beta_1^2\right) \frac{1}{\sqrt{2\pi}\sqrt{1-\rho^2}} \exp$$

$$\times \left[-\frac{1}{2}\left(\frac{\beta_2 - \rho\beta_1}{\sqrt{1-\rho^2}}\right)^2\right] d\beta_2\, d\beta_1 \tag{A6}$$

$$= \int_{\beta_{10}}^{\infty} \int_{\Delta(\beta_1)}^{\infty} \frac{1}{\sqrt{2\pi}} \exp\left(-\frac{1}{2}\beta_1^2\right) \frac{1}{\sqrt{2\pi}} \exp\left(-\frac{1}{2}\xi^2\right) d\xi\, d\beta_1$$

$$= \int_{\beta_{10}}^{\infty} \frac{1}{\sqrt{2\pi}} \exp\left(-\frac{1}{2}\beta_1^2\right) \Phi[-\Delta(\beta_1)]\, d\beta_1$$

where the transformed variables

$$\xi = \frac{\beta_2 - \rho\beta_1}{\sqrt{1-\rho^2}} \tag{A7}$$

$$\Delta(\beta_1) = \frac{\beta_{20} - \rho\beta_1}{\sqrt{1-\rho^2}} \tag{A8}$$

are defined.

To calculate this integral numerically, the following additional variable transformation is introduced:

$$\beta_1 = \frac{2}{1+\eta} + \beta_{10} - 1 \tag{A9}$$

$$'d\beta_1 = -\frac{2}{(1+\eta)^2}\, d\eta \tag{A10}$$

This will transform $\beta_1(\beta_{10}, \infty)$ to $\eta(1, -1)$ as

$$P(E_1E_2) = \frac{1}{\sqrt{2\pi}} \int_{-1}^{1} \frac{2}{(1+\eta)^2} e^{-(1/2)\beta_1^2} \Phi[-\Delta(\beta_1)]\, d\eta \tag{A11}$$

The integral is a properly behaved integral, such that Gaussian quadrature can be used to calculate the integral very accurately.

Acknowledgments

This research was sponsored by NASA Lewis Research Center under Contract NAS3-24389 (Program Manager, C. C. Chamis) through subcontract to Southwest Research Institute (Project Manager, Y.T. Wu). The authors gratefully acknowledge this support. The authors also acknowledge the technical discussions with K. Rajagopal of Rockwell International (Rocketdyne Division), which helped in the implementation of the example on system risk assessment.

References

[1]Cruse, T. A., Burnside, O. H., Wu, Y.-T., Polch, E. Z., and Dias, J. B., "Probabilistic Structural Analysis Methods for Select Space Propulsion System Structural Components (PSAM)," *Computers and Structures*, Vol. 29, No. 5, 1988, pp. 891–901.

[2]Ang, A. H-S., and Tang, W. H., *Probability Concepts in Engineering Design*, Vol. II, Wiley, New York, 1984.

[3]Wu, Y. T., and Wirsching, P. H., "New Algorithm for Structural Reliability Estimation," *Journal of Engineering Mechanics*, ASCE, Vol. 113, No. 9, 1987, pp. 1319–1336.

[4]Ditlevsen, O., "Narrow Reliability Bounds for Structural Systems," *Journal of Structural Mechanics*, Vol. 3, 1979, pp. 453–472.

[5]Wu, Y. T., Millwater, H. R., and Cruse, T. A., "An Advanced Probabilistic Structural Analysis Method for Implicit Performance Functions," *AIAA Journal*, Vol. 28, No. 9, 1990, pp. 1663–1669.

[6]Mahadevan, S., and Cruse, T. A., "An Advanced First-Order Method for System Reliability," *Proceedings of the Sixth ASCE Joint Specialty Conference on Probabilistic Mechanics and Structural and Geotechnical Reliability* (Denver, CO), American Society of Civil Engineers, New York, 1992, pp. 487–490.

[7]Mahadevan, S., Cruse, T. A., Huang, Q., and Mehta, S., "Structural Reanalysis for System Reliability Computation," *Reliability Technology*, Vol. AD-28, American Society of Mechanical Engineers, New York, 1992, pp. 169–187.

[8]Mahadevan, S., and Chamis, C. C., "Structural System Reliability Under Multiple Failure Modes," *Proceedings of the AIAA/ASME/ASCE/AHS/ASC 34th Structures, Structural Dynamics, and Materials Conference*, AIAA, Washington, DC, 1993, pp. 707–713.

[9]Hohenbichler, M., and Rackwitz, R., "First-Order Concepts in System Reliability," *Structural Safety*, Vol. 1, 1983, pp. 177–188.

[10]Ostergaard, D. F., and Hillberry, B. M., "Characterization of the Variability in Fatigue Crack Propagation Data," *Probabilistic Fracture Mechanics and Fatigue Methods*, ASTM STP 798, edited by J. M. Bloom and J. C. Ekvall, American Society for Testing and Materials, Philadelphia, PA, 1983, pp. 97–115.

[11]Cruse, T. A., Huang, Q., Mahadevan, S., and Mehta, S., "System Reliability and Analysis Research," Vols. I and II, Vanderbilt Univ., Rept. ME92-351-01, Nashville, TN, 1991.

[12]Wu, Y.-T., "An Adaptive Importance Sampling Method for Structural System Reliability Analysis," *Reliability Technology*, Vol. AD-28, American Society of Mechanical Engineers, New York, 1992, pp. 217–231.